

KINETICS OF THE DECOMPOSITION OF ORTHO HALOGENATED PHENOXY RADICALS

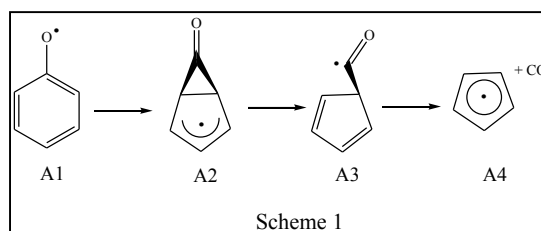
Mohammednoor Altarawneh*, Bogdan Z. Dlugogorski

School of Engineering and Information Technology, Murdoch University, Murdoch, WA 6150, Australia

*Corresponding author: Phone: (+61) 8 9360 7507; Email: M.Altarawneh@murdoch.edu.au

Introduction

Halogenated phenoxy radicals constitute the most potent precursors for the formation of polyhalogenated dibenzo-*p*-dioxins and dibenzofurans. Self-dimerisation of halogenated phenoxy occurs homogeneously in the gas phase (700 – 1000 K) or via catalytic-assisted reactions (500 – 700 K).¹ Halogenated phenoxy radicals form from their respective halogenated phenol molecules either through direct scission of hydroxyl OH bond or through bimolecular reactions. Other sources for the formation of halogenated phenoxy-type radicals include unimolecular rearrangements of brominated flame retardants and fissions of ether linkages in biomass constituents. Due to their electron-delocalised systems, substituted phenoxy (Phx) radicals resist oxidation initiated by addition of oxygen molecules. However, bimolecular coupling of substituted phenoxy radical represents a rather minor channel if compared with their unimolecular decomposition via the ring contraction/CO elimination mechanism. Previous theoretical work has indicated that unsubstituted Phx² radicals decompose into CO and cyclopentadienyl radicals (*cyc*-C₅H₅) through a three-step mechanism as Scheme 1 portrays. Oxidative decomposition of aromatic compounds, most notably at high temperature, follows the mechanism in Scheme 1. This is because, the addition of an oxygen molecule to a phenyl-type radical with a subsequent fission of the O-O bond results in the formation of A1-like radicals.



On the other hand, halogenated cyclopentadienyl radicals serve as major building blocks for the formation of halogenated naphthalene; and subsequently halogenated polyaromatic hydrocarbons (HPAHs). Shock tube experiments of Lin and Lin³ between 1010 – 1430 K and 0.5 – 0.9 atm established an overall rate constant for the unimolecular decomposition of Phx radical to be $k(T) = 2.50 \times 10^{11} \exp(-43\,900/RT) \text{ s}^{-1}$. To this end, our aim in this study is to provide kinetic parameters for the decomposition of *ortho*-chlorophenoxy (*o*-ClPhx) and *ortho*-bromophenoxy (*o*-BrPhx) radicals and contrast these parameters with analogous experimental and theoretical values of Phx radicals.

Computational Methodology

We carry out all structural optimisations and energy calculations with the aid of Gaussian09⁴ programme at the accurate composite method of CBS-QB3⁵. The CBS-QB3 method initially locates the minimum energy structure and computes its vibrational frequencies at the B3LYP/CBSB7 level before refining final energies through a series of single point energy calculations at higher theoretical levels. We calculate pressure-dependent reaction rate constants within the formalism of the RRKM/ME analysis as implemented in the Chemrate code.⁶ In these calculations, we deploy Lennard-Jones parameters of phenol, i.e., $\sigma = 4.5 \text{ \AA}$ and $\epsilon/k_B = 450.0 \text{ K}$ with the value of $\langle \Delta E \rangle_{\text{down}}$ equal to 200 cm^{-1} . We estimate time-dependent species profiles for one reaction using the recently developed MESMER code.⁷

Results and Discussions

Structures of the three radicals: Implications to formation of pre-dioxin intermediates

Self-condensation of the two halogenated phenoxy radicals leading to formation of pre-dioxins intermediates could potentially occur through

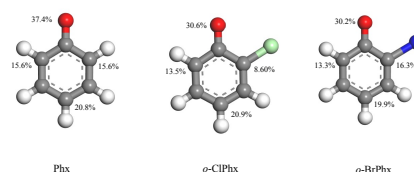


Figure 1: Spin densities on the three title radicals. Marginal spin densities appear on other atoms and are not shown.

their phenoxy O, as well as *ortho* and *para* carbon atoms. Thus, it is instrumental to gain an insight into the relative distribution of the radical character in phenoxy substituted radicals. Figure 1 shows optimised structures of the three phenoxy radicals along with their estimated spin densities. As Figure 1 depicts, the phenoxy O atom in the Phx radical holds more electron density than corresponding O atoms in *o*-ClPhx and *o*-BrPhx radicals. This suggests that, formation of ether-type pre-dioxin intermediates is likely to be more plausible during the self-dimerisation of Phx radicals in reference to that of the two halogenated phenoxy radicals. It is worthwhile noting that formation of pre-dioxin intermediates from halogenated phenoxy radicals occurs without reaction barriers; i.e., their formation is merely thermodynamically controlled.¹

The substituted *ortho* carbon in the *o*-ClPhx radical could be regarded as a slightly deficient radical site if compared with the corresponding carbon atom in the *o*-BrPhx radical, i.e. 8.6% versus 16.3%. As a consequence, coupling through the *ortho* carbon bearing a chlorine atom in the *o*-ClPhx radical is expected to be less thermodynamically driven than analogous coupling in the *o*-BrPhx radical. Clearly, assessing the influence of the spin densities on the relative abundance of pre-dioxin intermediates necessitates estimating equilibrium concentrations of these adducts at temperatures of interest and warrants further investigation.

Potential energy surface (PES) for the ring contraction/CO elimination mechanism

Figure 2 depicts PESs for the unimolecular decomposition of the three title radicals. PESs for the three radicals reveal that their energetic requirements are very similar; albeit, with some noticeable deviation for the *o*-BrPhx radical. For instance, activation enthalpies for transition states TS2 in case of Phx and *o*-ClPhx amount to 53.4 kcal/mol and 52.4 kcal/mol; i.e., slightly higher than the corresponding value for the *o*-BrPhx radical of 49.6 kcal/mol. An enthalpic barrier of TS2 signifies the overall impediment of the mechanism. In order to observe effects pertinent to the position of the halogen atom on energetics of Scheme 1, in Table 1, we enlist reaction ($\Delta_r H^\circ$) and activation (ΔH^\ddagger) enthalpies of the three steps for all monohalogenated phenoxy radicals.

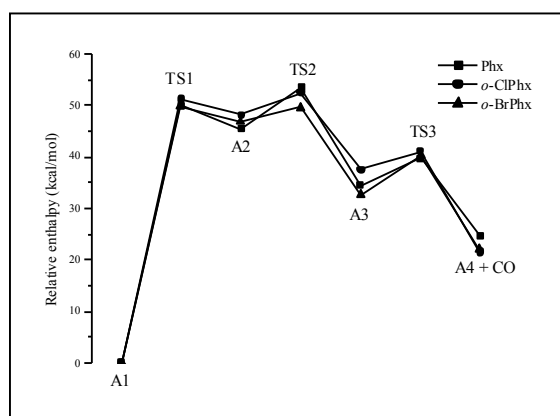


Figure 2: PESs for CO elimination from Phx, *o*-ClPhx and *o*-BrPhx radicals.

Table 1: Reaction ($\Delta_r H^\circ$) and activation (ΔH^\ddagger) enthalpies of the three steps in the ring contraction/CO elimination mechanism for monohalogenated phenoxy radicals. All values are in kcal/mol relative to A1.

	TS1	A2	TS2	A3	TS3	A4 + CO
Phx	50.0	45.5	53.4	34.4	39.8	24.7
<i>o</i> -ClPhx	51.2	48.1	52.4	37.5	41.1	21.6
<i>o</i> -BrPhx	49.8	46.8	49.6	32.7	40.4	22.0
<i>m</i> -ClPhx	48.9	44.9	53.6	34.3	38.5	21.0
<i>m</i> -BrPhx	48.7	44.7	53.4	34.6	39.8	21.5
<i>p</i> -ClPhx	52.8	47.5	55.1	35.6	42.0	22.6
<i>p</i> -BrPhx	53.4	46.9	54.6	35.2	41.0	22.7

As Table 1 shows, enthalpic barriers of TS2 for all monohalogenated phenoxy radicals, except that of *o*-BrPhx, reside within the very narrow range of 52.4 kcal/mol and 55.1 kcal/mol. This implies that the position of the halogen atom exerts a rather minor influence on the reaction barrier of the rate determining step of CO elimination from monohalogenated phenoxy radicals. It follows that, the reaction rate constant calculated in the next section for *ortho* monohalogenated phenoxy radicals should also be applicable to *meta* and *para* monohalogenated phenoxy radicals.

Apparent overall reaction rate constants at 1.0 atm

In their comprehensive kinetic analysis for CO elimination from Phx radical, Carstensen and Dean² demonstrated that deploying $A1 \rightarrow TS2 \rightarrow A4 + CO$ as a simplified overall reaction yields virtually the same rate constants when considering the three-step mechanism. Their calculated reaction rate constants at the high-pressure limit as well as at 1.0 atm match very well analogous experimental measurements. Similarly, in this work, we estimated the reaction rate constant for CO elimination from *o*-ClPhx and *o*-BrPhx radicals based on a simplified one-step mechanism. We first validated calculated kinetic parameters of Phx radical against corresponding experimental results before proceeding to estimate overall apparent reaction rate constants for the unimolecular decomposition of *o*-ClPhx and *o*-BrPhx. Figure 3 compares our calculated reaction rate constant at different pressures with corresponding experimental measurements. At 900 K, our computed rate constant at the high-pressure limit deviates from the two sets of experimental measurements by factors of 1.3 and 2.78. Our calculated values for phenoxy also coincides very well with the analogous theoretical predictions by Carstensen and Dean² obtained by using three approaches, employing MultiWell, UniMol and ChemDis packages. Table 2 gives Arrhenius parameters for CO elimination from *o*-ClPhx and *o*-BrPhx at 1.0 atm and at the high-pressure limit.

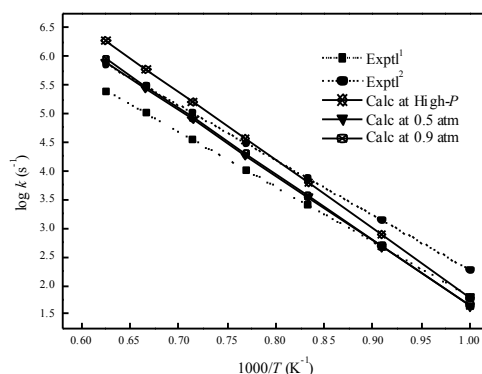


Figure 3: Comparison between calculated and experimental values for reaction rate constants of phenoxy \rightarrow CO + C₃H₅.

Table 2: Arrhenius parameters for CO elimination fitted in the temperature range of 400 to 1600 K.

	1 atm		High P	
	A (s ⁻¹)	E_a (cal/mol)	A (s ⁻¹)	E_a (cal/mol)
Phx	1.66×10^{13}	52 800	5.61×10^{13}	54 700
<i>o</i> -ClPhx	1.62×10^{12}	51 400	1.29×10^{14}	53 800
<i>o</i> -BrPhx	3.55×10^{12}	49 200	1.20×10^{13}	50 500

At 1 atm and between 700 – 1000 K (in relevance to homogenous formation of dioxins), unimolecular decomposition of the three title radicals takes place at very comparable rates. We estimate the lifetimes of Phx, *o*-ClPhx and *o*-BrPhx at 773.15 K and 1 atm to be 1.61 s, 6.69 s and 7.6 s, respectively. The relatively long

calculated lifetimes of the three radicals, in line with experimental measurements,⁸ permit these radicals to undergo bimolecular reactions leading to formation of halogenated dibenzo-*p*-dioxins and dibenzofurans. Overall, *ortho*-halogen substituents exert a rather minor influence on the overall kinetics of unimolecular reactions in reference to non-halogenated Phx radicals.

In Figure 4, we test the validity of using a simplified one-step reaction to describe the overall decomposition of halogenated phenoxy radicals. Due to the very shallow well-depths of A2 and A3 with respect to TS2 and TS3 (i.e. 4.3 kcal/mol and 3.6 kcal/mol, respectively in case of *o*-ClPhx radical), A1 transforms directly into A4 without any accumulation into A2 and A3 intermediates. As a consequence, the latter two adducts are absent from the time-dependent species profiles shown in Figure 4. At 1.0 atm and 900 K, we estimate conversions of A2 into A3 and A3 into A4 + CO to be very fast with rate constants of $6.10 \times 10^{12} \text{ s}^{-1}$ and $1.70 \times 10^8 \text{ s}^{-1}$, respectively. This finding reveals that A2 and A3 are very short-lived species and that the overall decomposition of halogenated phenoxy radicals could be effectively described by a simplified one-step reaction. In view of the very comparable enthalpic values in Table 2, we anticipate the unimolecular decomposition of all other monohalogenated phenoxy radicals to exhibit very similar behaviour to that depicted in Figure 4.

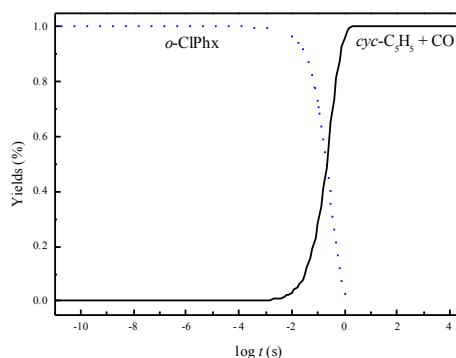


Figure 4: Time-dependent species profiles for the unimolecular decomposition of the *o*-ClPhx radical at 900 K and 1.0 atm.

Acknowledgments

This study has been supported by the Australian Research Council (ARC) as well as computational time grants from the Pawsey Computing Centre in Perth and the National Computational Infrastructure (NCI) in Canberra, Australia.

References

1. Altarawneh M, Dlugogorski BZ, Kennedy EM, Mackie JC. (2009); *Prog. Energy Combust Sci.* 35: 245-74.
2. Carstensen H, Dean A. (2012); *Int. J. Chem. Kinet.* 44:75-89.
3. Lin CY, Lin M. (1986); *J. Phys. Chem.* 90: 425-31.
4. Frisch MJ, et al. (2009), Gaussian09, Gaussian Inc, Wallingford CT.
5. Baboul AG, Curtiss LA, Redfern PC, Raghavachari K. (1999); *J. Chem. Phys.* 100: 7650-7657.
6. Mokrushin V. (2009), ChemRate, NIST, Gaithersburg.
7. Glowacki DR, Liang C, Morley C, Pilling MJ, Robertson SH. (2012); *J. Phys. Chem. A.* 116: 9545-9560.
8. Dellinger B. (2007). *Proc. Combust. Inst.* 31: 521-528.